# Structure and biochemical characterization of an adenylate kinase originating from the psychrophilic organism *Marinibacillus marinus*

Milya Davlieva and Yousif Shamoo*

Department of Biochemistry and Cell Biology, Rice University, 6100 Main Street MS-140, Houston, Texas, USA

Correspondence e-mail: shamoo@rice.edu

Adenylate kinases (AKs; EC 2.7.4.3) are essential members of the NMP kinase family that maintain cellular homeostasis by the interconversion of AMP, ADP and ATP. AKs play a critical role in adenylate homeostasis across all domains of life and have been used extensively as prototypes for the study of protein adaptation and the relationship of protein dynamics and stability to function. To date, kinetic studies of psychrophilic AKs have not been performed. In order to broaden understanding of extremophilic adaptation, the kinetic parameters of adenylate kinase from the psychrophile *Marinibacillus marinus* were examined and the crystal structure of this cold-adapted enzyme was determined at 2.0 Å resolution. As expected, the overall structure and topology of the psychrophilic *M. marinus* AK are similar to those of mesophilic and thermophilic AKs. The thermal denaturation midpoint of *M. marinus* AK (321.1 K) is much closer to that of the mesophile *Bacillus subtilis* (320.7 K) than the more closely related psychrophile *B. globisporus* (316.4 K). In addition, the enzymatic properties of *M. marinus* AK are quite close to those of the mesophilic AK and suggests that *M. marinus* experiences temperature ranges in which excellent enzyme function over a broad temperature range (293–313 K) has been retained for the success of the organism. Even transient loss of AK function is lethal and as a consequence AK must be robust and be well adapted to the environment of the host organism.

1. Introduction

Adenylate kinases (AKs) from a variety of organisms have proven to be excellent subjects for studies of molecular evolution (Counago *et al.*, 2006, 2008) and protein folding (Henzler-Wildman *et al.*, 2007; Whitford *et al.*, 2007, 2008; Bae *et al.*, 2008; Lu & Wang, 2008; Arora & Brooks, 2007; Bae & Phillips, 2004, 2006; Wolf-Watz *et al.*, 2004; Criswell *et al.*, 2003). AK homologs isolated from extremophiles have been used to elucidate the underlying basis of adaptation as well as to provide new insights for models of protein folding, dynamics and design (Bae *et al.*, 2008; Whitford *et al.*, 2007; Bae & Phillips, 2004; Criswell *et al.*, 2003; Nguyen *et al.*, 2008). AK (EC 2.7.4.3) regulates adenylate homeostasis (ATP + AMP ↔ 2ADP) and is essential for proper maintenance of the cellular energy charge ([ATP] + 0.5[ADP])/([ATP] + [ADP] + [AMP]) (Atkinson, 1968). In addition to its metabolic role, AK is a prototypical phosphoryl-transfer enzyme and as such is a good model for the critically important family of kinases implicated in cellular signaling. AK can be broadly described as having a LID domain (residues 128–159) and a CORE (residues 1–30, 60–127 and 160–217) domain.

High-resolution structures exist for representative members of both monomeric and trimeric forms of AK (Bae & Phillips, 2004; Criswell *et al.*, 2003; Vonrhein *et al.*, 1998). Within the monomeric AK family, structures have been determined of AKs from the thermophile *Geobacillus stearothermophilus* (AK$_{GS}$; Berry & Phillips, 1998), the mesophiles *Bacillus subtilis* (AK$_{BS}$; Bae & Phillips, 2004) and *Escherichia coli* (AK$_{EC}$; Muller & Schulz, 1998), and the psychrophile *B. globisporus* (AK$_{BG}$; Bae & Phillips, 2004). While structures across a broad temperature range are represented, the enzyme kinetics for a psychrophilic AK have not been determined. We have solved the
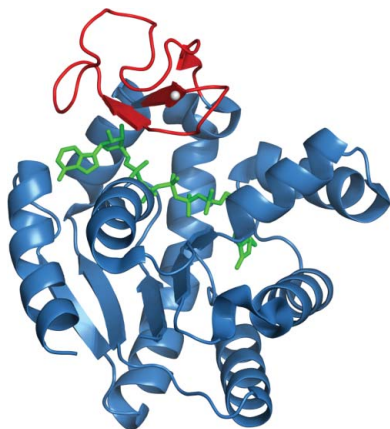
structure of *Marinibacillus marinus* AK (AK$_{MM}$) at 2.0 Å resolution and have also determined its stability and temperature-dependent kinetic parameters. The structure and kinetic parameters suggest that AK$_{MM}$ has properties that are consistent with an organism that has optimized enzymatic performance over a broader temperature range than the related psychrophile *B. globisporus*.

M. marinus is a subspecies of *B. globisporus* (their AKs are 72.8% identical) that was originally isolated from sediment in the North East Atlantic as an obligate halophile with an optimum growth range of 285–296 K (Yoon *et al.*, 2001; Rüger & Richter, 1979; Rüger *et al.*, 2000). Structure–function studies on psychrophilic AKs are quite limited, but comparative studies of mesophilic and thermophilic enzymes suggest strong correlations between protein dynamics and function that are tuned adaptively towards optimal enzyme performance within the environmental niche of the host organism (Counago *et al.*, 2006; Henzler-Wildman *et al.*, 2007; Bae & Phillips, 2004). While no kinetic parameters have been measured for AK$_{BG}$, the total enzyme activity as a function of temperature has been examined and shows a distinct maximum at 308 K, while AK$_{MM}$ has a much broader activity range that is more similar to those of the mesophilic AKs. Although *M. marinus* AK has kinetic characteristics that are similar to those of the mesophilic AK$_{BS}$, the K_M for both ATP and AMP shows less temperature-dependence, making this a robust enzyme over temperature ranges below the denaturation temperature of the protein and over the entire growth range of the host organism.

2. Materials and methods

Pyruvate kinase, L-lactate dehydrogenase, phosphoenolpyruvate, β-nicotinamide adenine dinucleotide, reduced disodium salt (NADH), adenosine 5′-triphosphate sodium salt (ATP), adenosine 5′-monophosphate disodium salt (AMP) and P^1,P^5-di(adenosine-5′)-pentaphosphate pentasodium salt (AP5A) were purchased from Sigma–Aldrich.

2.1. Cloning, expression and purification of AK$_{MM}$

The gene encoding *M. marinus* adenylate kinase (AY690426) was amplified from genomic DNA (ATCC 29841) and subcloned into pET11a as pET11a-AK$_{MM}$. *E. coli* Rosetta cells containing plasmid pET11a-AK$_{MM}$ were grown at 310 K in LB medium containing 50 µg ml^{-1} carbenicillin and 25 µg ml^{-1} chloramphenicol to mid-log phase (OD$_{600}$ = 0.6–0.7). Prior to induction, the temperature was reduced to 303 K. Expression of AK$_{MM}$ was induced by the addition of isopropyl β-D-1-thiogalactopyranoside to 1 mM and the culture was incubated for an additional 17 h. Cells were harvested by centrifugation and the cell lysate was cleared and loaded onto a HiTrap Q-XL Sepharose anion-exchange chromatography column and eluted with a gradient from 0 to 0.5 M NaCl. The pooled fractions were concentrated, dialyzed against 50 mM Tris pH 7.5, 50 mM NaCl, 1 mM MgCl$_2$, 0.1 mM EDTA, 0.3 mM DTT and passed over a column containing Affi-Gel Blue resin (Bio-Rad). The absorbed protein was eluted using a gradient from 0.1 to 2.5 M NaCl. Following concentration, AK$_{MM}$ was passed over a HiLoad 16/60 Superdex-200 column (Amersham Biosciences). The sample purity was assessed by SDS–PAGE and found to be >95%.

2.2. AK$_{MM}$ activity assays

Kinetic parameters for the formation of ATP by AK$_{MM}$ were determined at 293, 303 and 313 K by a continuous assay (Girons *et al.*, 1987; Vieille *et al.*, 2003). The reaction mixture consisted of reaction buffer (25 mM phosphate buffer pH 7.2, 5 mM MgCl$_2$, 65 mM KCl, 0.06 mM NADH, 0.1 mM phosphoenolpyruvate, five units of both lactate dehydrogenase and pyruvate kinase, 1.4 mM AMP) and various ATP concentrations (0.1, 0.5, 1, 5, 10, 50, 100 and 500 µM). The mixture was kept at the desired temperature for 5 min in a water bath prior to addition of AK$_{MM}$ to a final concentration of 9 nM. A sample of the reaction buffer without the addition of AK$_{MM}$ was used as a control at each temperature. The amount of ADP produced was estimated from the conversion of NADH to NAD$^+$ as indicated by the absorbance at 340 nm (molar extinction coefficient $\varepsilon_{340\,nm}$ = 6200 M^{-1} cm^{-1}), subtracting the amount of NADH consumed from the NADH concentration for the control reaction. The kinetic parameters (K_M and V_{max}) were estimated in an initial velocity *versus* [ATP] plot by fitting the data to the Michaelis–Menten equation using *Kaleidagraph* v.3.51 (Synergy Software). The data shown are the average of two experiments performed in triplicate at each temperature. The enzyme activity of AK$_{MM}$ was also determined at 293, 303 and 313 K for the formation of AMP by varying the AMP concentration (0.1, 0.5, 1, 5, 10, 50, 100 and 500 µM) and maintaining a constant ATP concentration (1.4 mM) using the continuous assay described previously.

2.3. Thermal unfolding (T_m) of AK$_{MM}$

The thermal stability of AK$_{MM}$ and of the complex of AK$_{MM}$ with the transition-state analog AP5A were measured by changes in ellipticity (Jasco J-815 CD) at 220 nm as a function of temperature (0.5° min^{-1}). To minimize the error arising from baseline corrections, the thermal unfolding midpoint (T_m) was calculated using the first derivative of the CD signal *versus* temperature (John & Weeks, 2000). The first derivative was obtained using a simple differential of the CD signal [$f(T) = \Delta CD/\Delta T$]. The position of the peak maximum was used to determine the thermal unfolding midpoint (T_m). Data were acquired in 10 mM potassium phosphate pH 7.2, 65 mM KCl and then converted into a plot of fraction unfolded *versus* temperature. Scans were performed from 293 to 363 K for AK$_{MM}$ and from 293 to 358 K for the complex with AP5A (100 µM). The data shown are the average of two independent experiments performed in triplicate.

2.4. Crystallization and structure determination of AK$_{MM}$

Preliminary AK$_{MM}$ crystallization trials were performed by the sitting-drop vapour-diffusion method using a sparse-matrix crystallization approach (Jancarik & Kim, 1991). 0.5 µl protein solution (15 mg ml^{-1}) with 9 mM AP5A in 10 mM HEPES pH 7.0 and 0.5 µl mother liquor were mixed in a 96-well plate using a Hydra II Plus One crystallization robot (Matrix Technology) and incubated at 283 K. The first crystals of AK$_{MM}$ were obtained in 1.6 M sodium citrate pH 6.5. This condition was successively modified using streak-seeding with crushed crystals and additive screening, resulting in crystals that were suitable for data collection. The final crystallization condition was 1.5 M sodium citrate pH 6.5, 150 mM sodium chloride, 0.5% *n*-dodecyl-*N*,*N*-dimethylamine-*N*-oxide at 283 K.

Crystals of AK$_{MM}$ were passed briefly through cryoprotectant solutions consisting of 1.5 M sodium citrate pH 6.5, 150 mM sodium chloride, 0.5% *n*-dodecyl-*N*,*N*-dimethylamine-*N*-oxide supplemented with 5, 10, 15 and 20%(*v*/*v*) ethylene glycol. Diffraction data were collected to 2.0 Å resolution on a Rigaku R-AXIS IV^{++} image-plate detector system with Varimax HF optics. All data were collected at 100 K using a nitrogen cryostream. The crystals belonged to space group *C*2, with unit-cell parameters a = 92.6, b = 46.5, c = 62.7 Å, $\alpha = \gamma$ = 90.0, β = 98.7°. The data were processed and merged using the program *d*TREK (Pflugrath, 1999).

The structure of AK_{MM} was solved by molecular replacement with the program *Phaser* from the *CCP*4 suite (Collaborative Computational Project, Number 4, 1994) using only the protein coordinates of AK_{BG} (PDB code 1s3g) as a search model (Bae & Phillips, 2004). The initial solution suggested the presence of one monomer per asymmetric unit, consistent with a Matthews coefficient of 2.78 $Å^3 Da^{-1}$ (56% solvent). The molecular-replacement solution was further confirmed by the initial composite omit maps generated using *CNS* (Brünger *et al.*, 1998), which clearly indicated strong electron density for AP5A and the structural zinc ion that were not included in the original search model. Refinement (20.0–2.0 Å) was carried out in *REFMAC*5 (Murshudov *et al.*, 1997) using standard restraints. After iterative refinement and model building, water molecules were added using the *Coot* find water function in *REFMAC*5. The AK_{MM} model was refined to convergence, resulting in an R factor of 18.0% and an

R_{free} of 22.6% to 2.0 Å resolution. Ramachandran plots and root-mean-square deviations from ideality for bond angles and lengths for AK_{MM} were determined using *PROCHECK* v.3.5 (Laskowski *et al.*, 1996) and the structure-validation program *MolProbity* (Davis *et al.*, 2007). All figures containing molecular structures were generated using *PyMOL* (DeLano, 2002) and *CCP4MG* (Potterton *et al.*, 2002, 2004). The structure of AK_{MM} has been deposited in the RCSB Protein Data Bank with code 3fb4.

3. Results

3.1. Enzyme kinetics for AK_{MM}

Kinetic parameters for the utilization of ATP and AMP were determined at 293, 303 and 313 K for AK_{MM} using a continuous assay
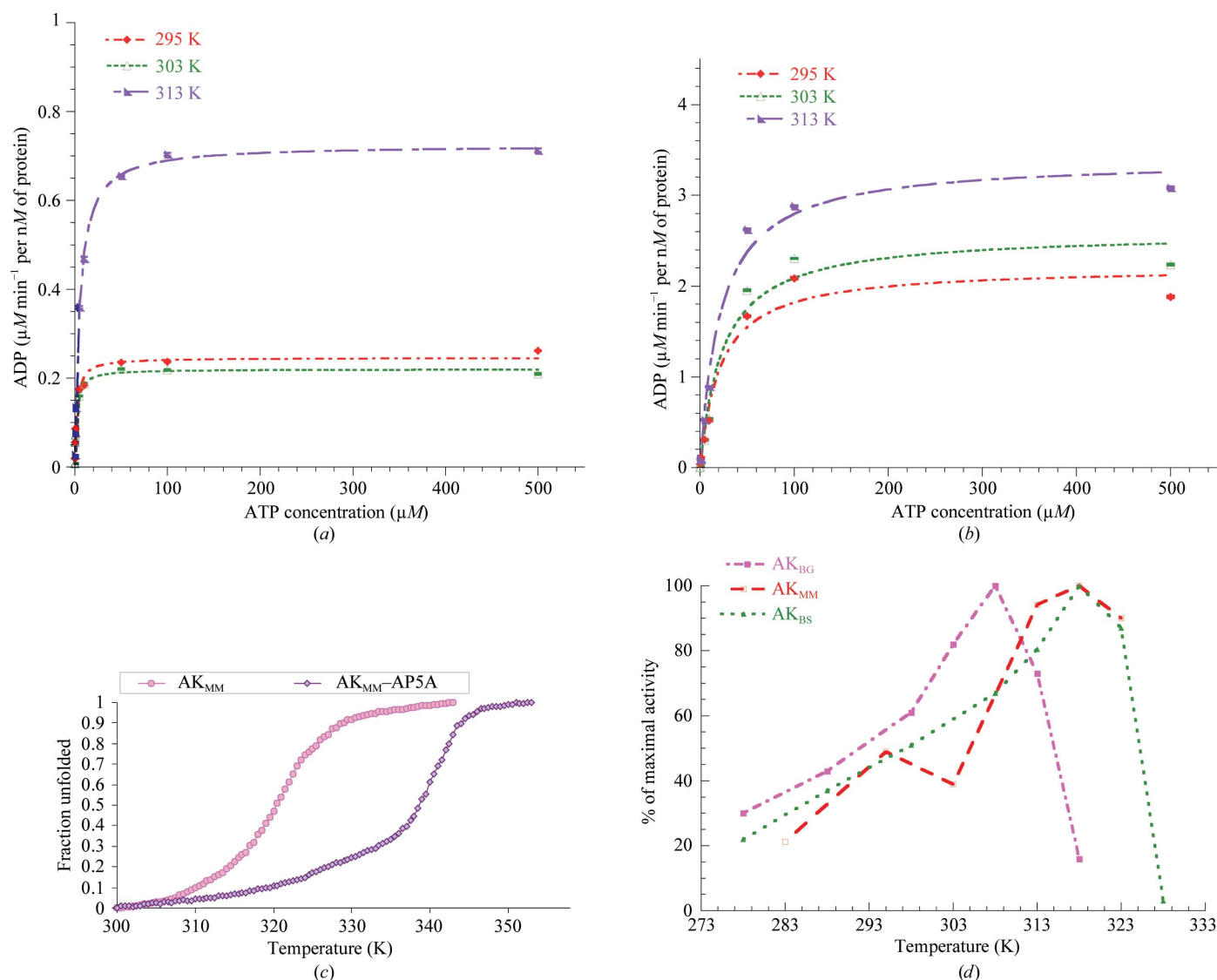

Figure 1
(*a*) ATP-dependent reaction kinetics for the production of ADP by AK_{MM} from 293 to 313 K. ATP was used as the variable substrate at concentrations of 0.1, 0.5, 1, 5, 10, 50, 100 and 500 µ*M* at each temperature. The concentrations of AK_{MM} (9 n*M*) and MgAMP (1400 µ*M*) were kept constant. The kinetic constants determined from these experiments are summarized in Table 1. (*b*) AMP-dependent reaction kinetics for the production of ADP by AK_{MM} from 293 to 313 K. AMP was used as the variable substrate at concentrations of 0.1, 0.5, 1, 5, 10, 50, 100 and 500 µ*M* at each temperature. The concentrations of AK_{MM} (9 n*M*) and MgATP (1400 µ*M*) were kept constant. The kinetic constants determined from these experiments are summarized in Table 1. (*c*) Thermal denaturation midpoints (T_m) of AK_{MM} and the AK_{MM}–AP5A complex from circular dichroism. The midpoint of the transition for unfolding of AK_{MM} at 20 µ*M* occurs at 321.1 K, while the midpoint of unfolding for the AK_{MM}–AP5A complex is 340.6 K, 19.5 K higher than for the free protein. (*d*) Temperature profile for the activity of *M. marinus* and *Bacillus* AKs. The temperature–activity profile for AK_{MM} has a much broader temperature range that is more similar to that of the mesophilic AK. The data for *B. globisporus* and *B. subtilis* AKs were taken from Bae & Phillips (2004).

Table 1
Kinetic parameters for *M. marinus* AK at various temperatures.

Temperature (K)	K_M (μM)		V_{max} (μM min^{-1} per nM of protein)	
	ATP	AMP	ATP	AMP
295	2.0 ± 0.3	21.4 ± 6.7	0.24 ± 0.01	2.2 ± 0.2
303	1.8 ± 0.2	24.0 ± 7.0	0.22 ± 0.01	2.6 ± 0.2
313	5.0 ± 0.3	21.6 ± 4.0	0.72 ± 0.01	3.4 ± 0.2

(Girons *et al.*, 1987; Vieille *et al.*, 2003). The temperature-dependence of the steady-state kinetic parameters (K_M and V_{max}) for ATP are shown in Fig. 1(*a*) and summarized in Table 1. AK$_{MM}$ displayed a fairly constant V_{max} over the range 293–303 K but a modest twofold increase from 295 to 313 K. The K_M values increased slightly over the same temperature range. The reaction patterns of AK$_{MM}$ for AMP at the indicated temperatures are shown in Fig. 1(*b*) and are summarized in Table 1. The temperature-dependence of K_M for AMP utilization was less than that of ATP, but the overall K_M for ATP (2–5 μM) is consistently lower than that for AMP (21–23 μM). The apparent difference in the observed k_{cat} for ATP and AMP may be the result of AMP inhibition at higher concentrations, as AMP is able to bind at the ATP-binding site (Sheng *et al.*, 1999).

3.2. Thermal denaturation followed by circular dichroism (CD)

Thermal stability was assessed using CD by following the changes in molar ellipticity with increasing temperature at 220 nm. As shown in Fig. 1(*c*), the midpoint of the transition for AK$_{MM}$ unfolding occurs at 321.1 K. CD experiments at concentrations of 2, 20 and 40 μM showed no concentration-dependence, which is consistent with the expected monomeric solution state. The stability of the ligand-bound closed conformation was estimated in the presence of 100 μM AP5A. It has previously been shown that AK$_{BG}$, AK$_{BS}$ and AK$_{GS}$ are greatly stabilized when bound to AP5A (Counago *et al.*, 2008; Bae & Phillips,

2004). Likewise, the midpoint of unfolding for AK$_{MM}$–AP5A is 19.5 K higher than that of the free protein.

3.3. Structural overview of AK$_{MM}$

The overall structure and topology of AK$_{MM}$ closely resemble those of AK$_{BG}$, AK$_{BS}$ and AK$_{GS}$, consistent with the strong sequence identity (72.8, 70.5 and 71.9% respectively) observed across this family of proteins (Fig. 2). Like other AKs, AK$_{MM}$ is a member of the α/β class, with a central β-sheet region surrounded by several α-helices that produce the characteristic AMP-binding, LID and CORE domains. Primary sequence alignment of the two most closely related family members, AK$_{MM}$ and AK$_{BG}$, shows that the C-terminal region (residues 184–216) is the most divergent. AKs from Gram-positive species including AK$_{MM}$ also contain a conserved-sequence zinc-binding motif (Cys-X_2-Cys-X_{16}-Cys-X_2-Cys/Asp; Fig. 3*a*; Bae & Phillips, 2004; Gilles *et al.*, 1994; Glaser *et al.*, 1992).

The crystal structure of AK$_{MM}$ was solved to a resolution of 2.0 Å and then refined to an R factor of 18.0% and an R_{free} of 22.6% (Table 2). AK$_{MM}$ was crystallized with the inhibitor AP5A bound to the active site. Superimposition of the C$^\alpha$ atoms of AK$_{MM}$ and AK$_{BG}$ shows that the structures are very similar, with an overall r.m.s.d. of 0.58 Å. A comparison of temperature factors suggests that AK$_{MM}$ (2.0 Å resolution; average main-chain B factor of 16.4 Å^2) is well ordered compared with AK$_{BG}$ (2.25 Å resolution; average main-chain B factor of 49.5 Å^2) and AK$_{BS}$ (1.90 Å resolution; average main-chain B factor of 27.7 Å^2), although the static disorder of the crystal also contributes to this. In order to analyze the flexibility of these enzymes and minimize the issues associated with crystal quality, data collection or refinement, the relative B factors were calculated by taking the mean B factor of every residue and dividing it by the mean B factor of the whole protein (Violot *et al.*, 2005). In this analysis, about 55% of the residues in AK$_{BG}$ showed higher relative B factors than those in AK$_{MM}$, whereas only 10% of the residues
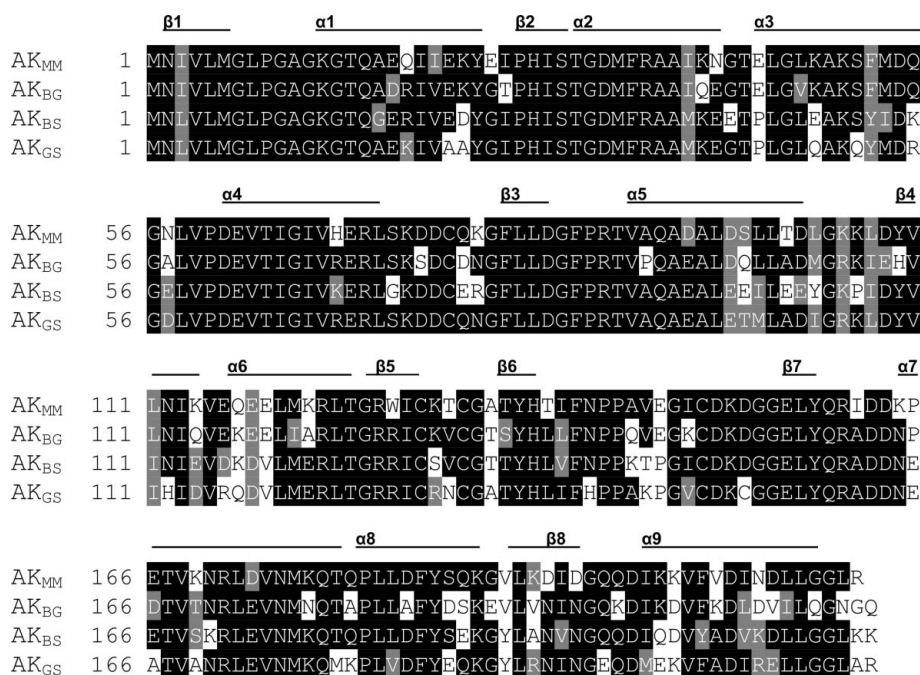

Figure 2
Primary sequence alignment of *M. marinus* AK and *Bacillus* AKs. The sequences were aligned using the program *ClustalW* and represented using the program *BOXSHADE* (Thompson *et al.*, 1994). AK$_{MM}$ shares high amino-acid sequence identity with other *Bacillus* AKs, including those of the psychrophile *B. globisporus* (AK$_{BG}$; 72.8%), the mesophile *B. subtilis* (AK$_{BS}$; 70.5%) and the thermophile *G. stearothermophilus* (AK$_{GS}$; 71.9%).

displayed a lower relative temperature factor. These results suggested an increase in the flexibility of AK_{BG}, which in general correlates with the lower thermostability. In contrast, the relative B factors for AK_{BS} and AK_{GS} showed a significantly smaller number of residues with higher flexibility and a larger number with lower flexibility, consistent with their thermostability (46% higher and 25% lower for AK_{BS} and
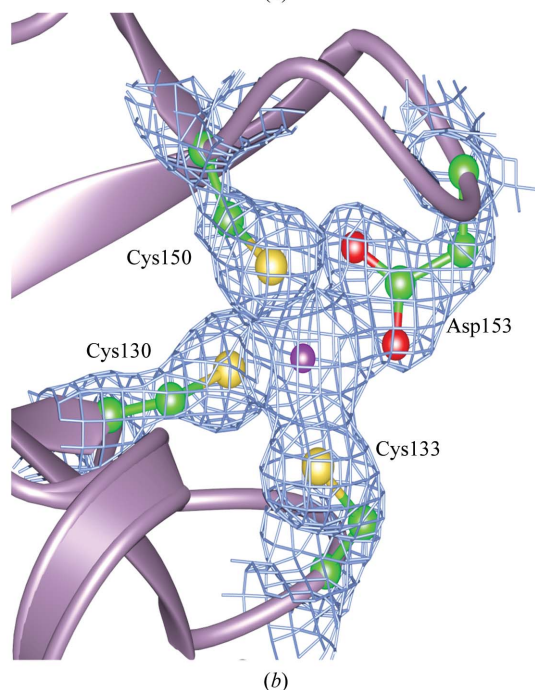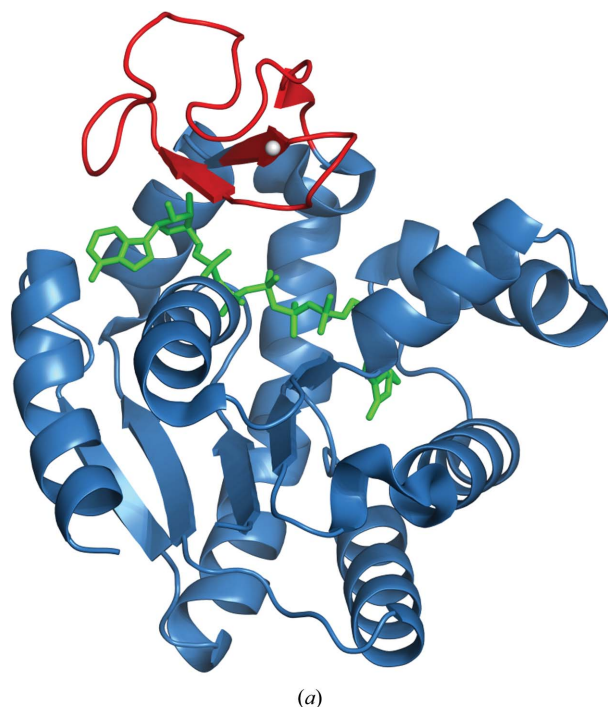

(a)

(b)

Figure 3
(a) Structure of psychrophilic *M. marinus* AK. The bound Zn^{2+} ion is shown as a gray sphere in the LID domain of the enzyme. The bound AP5A molecule (green) spans the active site of the enzyme. The LID domain (red) is in the fully closed conformation. (b) Electron density for bound Zn^{2+} and surrounding ligands in AK_{MM}. The coordination of Zn^{2+} (purple) to AK_{MM} is clearly visible in the $(2F_o - F_c)$ σ_A-weighted electron-density map contoured at 1.5σ. The bound Zn^{2+} is coordinated to Cys130, Cys133, Cys150 and Asp153 in a manner similar to that in other Gram-positive AKs.

Table 2
Data-collection and refinement statistics for the *M. marinus* AK structure.

Values in parentheses are for the last shell.

Data collection	
Wavelength (Å)	1.5418
Resolution (Å)	33.42–2.00 (2.07–2.00)
Space group	$C2$
Molecules per ASU	1
Unit-cell parameters (Å, °)	$a = 92.6$, $b = 46.5$, $c = 62.7$, $\alpha = \gamma = 90.0$, $\beta = 98.7$
Unique reflections	17786 (1713)
Average redundancy	2.81 (2.46)
Completeness (%)	98.7 (96.9)
R_{merge}† (%)	2.9 (8.0)
Output $\langle I/\sigma(I)\rangle$	24.0 (9.4)
Refinement	
R_{work}‡ (%)	18.0 (21.2)
R_{free}§ (%)	22.6 (27.0)
R.m.s.d.¶ from ideality	
Bonds (Å)	0.019
Angles (°)	1.9
Average B factor (Å^2)	19.12
Wilson plot B factor (Å^2)	7.9
Ramachandran plot††	
Most favored regions (%)	96.7
Additional allowed regions (%)	3.3
PDB code	3fb4

† $R_{merge} = \sum_{hkl} \sum_i |I_i(hkl) - \langle I(hkl)\rangle| / \sum_{hkl} \sum_i I_i(hkl)$, where $I(hkl)$ is the measured intensity for reflections with indices hkl. ‡ $R_{work} = \sum_{hkl} |F_o - F_c| / \sum_{hkl} |F_o|$ for all data with $F_o > 2\sigma(F_o)$, excluding data used to calculate R_{free}. § $R_{free} = \sum_{hkl} |F_o - F_c| / \sum_{hkl} |F_o|$ for all data with $F_o > 2\sigma(F_o)$ that were excluded from refinement. ¶ Root-mean-square deviation. †† Calculated using *PROCHECK* (Laskowski *et al.*, 1996).

39% higher and 25% lower for AK_{GS}). In addition, the average local structural entropy (LSE) values of AK_{BG}, AK_{MM} and AK_{BS} were calculated for the CORE domains (Chan *et al.*, 2004). AK_{MM} has a lower average LSE value than that of AK_{BG}, which correlates with the higher thermostability and highlights the importance of entropy in the stability of protein structures.

The LID domain of AK_{MM} is fully closed, as observed in the structures of AK_{BS} and AK_{BG}. The bound metal modeled as a Zn^{2+} is clearly evident in the LID domain of our structure and is coordinated to Cys130, Cys133, Cys150 and Asp153 (Fig. 3b). The carboxylate of Asp153 shows a bidentate coordination to the Zn^{2+}. As observed in AK_{BG}, one of the interactions from the O atom of the bidentate ligand Asp153 is longer than the other (Bae & Phillips, 2004; Alberts *et al.*, 1998). The inhibitor AP5A is bound occupying both the ATP/ADP and AMP/ADP sites, as has been observed in the AK_{BG}, AK_{BS} and AK_{GS} complexes.

4. Discussion

The AK family of proteins has emerged as a prototype for the study of protein folding, adaptive protein evolution, dynamics and design (Counago *et al.*, 2006, 2008; Henzler-Wildman *et al.*, 2007; Whitford *et al.*, 2007, 2008; Bae *et al.*, 2008; Lu & Wang, 2008; Arora & Brooks, 2007; Bae & Phillips, 2004, 2006; Wolf-Watz *et al.*, 2004; Criswell *et al.*, 2003; Nguyen *et al.*, 2008). AKs have been isolated from a range of extremophilic and temperate organisms and serve as a living record of adaptation, providing insights into protein evolution. In order to expand our understanding of extremophilic adaptation, we have determined the structure and elucidated the enzymatic properties of an AK from the psychrophile *M. marinus*. Surprisingly, the enzymatic properties of AK_{MM} are quite close to those of mesophiles such as *B. subtilis* and this suggests that *M. marinus* experiences temperature ranges in which excellent enzyme function over a broad temperature range (293–313 K) has been retained for the success of the organism.

structural communications

We compared the activity profile and structure of AK_{MM} with those of *B. globisporus* and *B. subtilis*. *M. marinus* is a closely related psychrophilic subspecies of *B. globisporus* and therefore we expected AK_{MM} to have quite comparable properties and structure to those of AK_{BG}. Although no detailed kinetics are available for the psychrophilic AK_{BG}, Bae & Phillips (2004) showed that the total activity of AK_{BG} was maximal at 308 K and decreased by ~30% from 308 to 313 K. AK_{MM} shows no loss in activity over the same range (Fig. 1*d*). In addition, the denaturation temperature of AK_{MM} (321.1 K) is quite close to that of AK_{BS} (320.7 K) (Bae & Phillips, 2004; our data). The relative magnitude of the K_M for ATP (2–5 µ*M*) is about tenfold lower than that for AMP (21–23 µ*M*), while those of AK_{BS} are nearly equal over a comparable temperature range (~10 and 11–26 µ*M*, respectively; Counago *et al.*, 2008). The K_M for AMP of AK_{MM} displayed less temperature-dependence than that of AK_{BS}, although in the case of AK_{BS} only a modest threefold change is observed over a comparable temperature range (293–313 K; Counago *et al.*, 2008).

Our findings suggest that AK_{MM} is a broad-range adenylate kinase that in many respects is more consistent with a mesophilic enzyme than might have been expected from previous work on the related psychrophilic *B. globisporus* AK_{BG}. *M. marinus* grows over a slightly broader temperature range (274–302 K) than *B. globisporus* (271–296 K) and suggests that the organism may require an AK with a broader functional range in order to deal with a more challenging environment. Previous work has shown that even transient loss of AK function in cells leads to an irreversible loss of viability (Counago & Shamoo, 2005) and therefore AK function may be well buffered for the entire range of temperatures an organism might experience in nature.

References

Alberts, I. L., Nadassy, K. & Wodak, S. J. (1998). *Protein Sci.* **7**, 1700–1716.

Arora, K. & Brooks, C. L. (2007). *Proc. Natl Acad. Sci. USA*, **104**, 18496–18501.

Atkinson, D. E. (1968). *Biochemistry*, **7**, 4030–4034.

Bae, E., Bannen, R. M. & Phillips, G. N. Jr (2008). *Proc. Natl Acad. Sci. USA*, **105**, 9594–9597.

Bae, E. & Phillips, G. N. Jr (2004). *J. Biol. Chem.* **279**, 28202–28208.

Bae, E. & Phillips, G. N. Jr (2006). *Proc. Natl Acad. Sci. USA*, **103**, 2132–2137.

Berry, M. B. & Phillips, G. N. Jr (1998). *Proteins*, **32**, 276–288.

Brünger, A. T., Adams, P. D., Clore, G. M., DeLano, W. L., Gros, P., Grosse-Kunstleve, R. W., Jiang, J.-S., Kuszewski, J., Nilges, M., Pannu, N. S., Read, R. J., Rice, L. M., Simonson, T. & Warren, G. L. (1998). *Acta Cryst.* D**54**, 905–921.

Chan, C. H., Liang, H. K., Hsiao, N. W., Ko, M. T., Lyu, P. C. & Hwang, J. K. (2004). *Proteins*, **57**, 684–691.

Collaborative Computational Project, Number 4 (1994). *Acta Cryst.* D**50**, 760–763.

Counago, R., Chen, S. & Shamoo, Y. (2006). *Mol. Cell*, **22**, 441–449.

Counago, R. & Shamoo, Y. (2005). *Extremophiles*, **9**, 135–144.

Counago, R., Wilson, C. J., Pena, M. I., Wittung-Stafshede, P. & Shamoo, Y. (2008). *Protein Eng. Des. Sel.* **21**, 19–27.

Criswell, A. R., Bae, E., Stec, B., Konisky, J. & Phillips, G. N. Jr (2003). *J. Mol. Biol.* **330**, 1087–1099.

Davis, I. W., Leaver-Fay, A., Chen, V. B., Block, J. N., Kapral, G. J., Wang, X., Murray, L. W., Arendall, W. B. III, Snoeyink, J., Richardson, J. S. & Richardson, D. C. (2007). *Nucleic Acids Res.* **35**, W375–W383.

DeLano, W. L. (2002). *The PyMOL Molecular Graphics System.* DeLano Scientific, San Carlos, California, USA.

Gilles, A. M., Glaser, P., Perrier, V., Meier, A., Longin, R., Sebald, M., Maignan, L., Pistotnik, E. & Bârzu, O. (1994). *J. Bacteriol.* **176**, 520–523.

Girons, I. S., Gilles, A. M., Margarita, D., Michelson, S., Monnot, M., Fermandjian, S., Danchin, A. & Barzu, O. (1987). *J. Biol. Chem.* **262**, 622–629.

Glaser, P., Presecan, E., Muriel, D., Witold, K., Surewicz, W. K., Mantsch, H. H., Barzu, O. & Gilles, A. N. (1992). *Biochemistry*, **31**, 3038–3043.

Henzler-Wildman, K. A., Lei, M., Thai, V., Kerns, J. S., Karplus, M. & Kern, D. (2007). *Nature (London)*, **450**, 913–916.

Jancarik, J. & Kim, S.-H. (1991). *J. Appl. Cryst.* **24**, 409–411.

John, D. M. & Weeks, K. M. (2000). *Protein Sci.* **9**, 1416–1419.

Laskowski, R. A., Rullmann, J. A., MacArthur, M. W., Kaptein, R. & Thornton, J. M. (1996). *J. Biomol. NMR*, **8**, 477–486.

Lu, Q. & Wang, J. (2008). *J. Am. Chem. Soc.* **130**, 4772–4783.

Muller, C. W. & Schulz, G. E. (1998). *J. Mol. Biol.* **202**, 909–912.

Murshudov, G. N., Vagin, A. A. & Dodson, E. J. (1997). *Acta Cryst.* D**53**, 240–255.

Nguyen, P. Q., Liu, S., Thompson, J. C. & Silberg, J. J. (2008). *Protein Eng. Des. Sel.* **21**, 303–310.

Pflugrath, J. W. (1999). *Acta Cryst.* D**55**, 1718–1725.

Potterton, E., McNicholas, S., Krissinel, E., Cowtan, K. & Noble, M. (2002). *Acta Cryst.* D**58**, 1955–1957.

Potterton, L., McNicholas, S., Krissinel, E., Gruber, J., Cowtan, K., Emsley, P., Murshudov, G. N., Cohen, S., Perrakis, A. & Noble, M. (2004). *Acta Cryst.* D**60**, 2288–2294.

Rüger, H. J., Fritze, D. & Sproer, C. (2000). *Int. J. Syst. Evol. Microbiol.* **50**, 1305–1313.

Rüger, H. J. & Richter, G. (1979). *Int. J. Syst. Bacteriol.* **29**, 196–203.

Sheng, X. R., Li, X. & Pan, X. M. (1999). *J. Biol. Chem.* **274**, 22238–22242.

Thompson, J. D., Higgins, D. G. & Gilbson, T. J. (1994). *Nucleic Acids Res.* **22**, 4673–4680.

Vieille, C., Krishnamurthy, H., Hyun, H. H., Savchenko, A., Yan, H. & Zeikus, J. G. (2003). *Biochem. J.* **372**, 577–585.

Violot, S., Aghajari, N., Czjzek, M., Feller, G., Sonan, G. K., Gouet, P., Gerday, C., Haser, R. & Receveur-Brechot, V. (2005). *J. Mol. Biol.* **348**, 1211–1224.

Vonrhein, C., Bonisch, H., Schafer, G. & Schulz, G. E. (1998). *J. Mol. Biol.* **282**, 167–179.

Whitford, P. C., Gosavi, S. & Onuchic, J. N. (2008). *J. Biol. Chem.* **283**, 2042–2048.

Whitford, P. C., Miyashita, O., Levy, Y. & Onuchic, J. N. (2007). *J. Mol. Biol.* **366**, 1661–1671.

Wolf-Watz, M., Thai, V., Henzler-Wildman, K. A., Hadjipavlou, G., Eisenmesser, E. Z. & Kern, D. (2004). *Nature Struct. Mol. Biol.* **11**, 945–949.

Yoon, J. H., Weiss, N., Lee, K. C., Lee, I. S., Kang, K. H. & Park, Y. H. (2001). *Int. J. Syst. Evol. Microbiol.* **51**, 2087–2093.